

Wave Propagation in Layered Cylindrical Structures Using Finite Element and Wave Tracing Analysis*

Sachiko SUEKI**, Samaan G. LADKANY** and Brendan J. O'TOOLE***

** Department of Civil and Environmental Engineering, University of Nevada, Las Vegas
4505 Maryland Parkway, Las Vegas, NV, 89154-4015, USA
E-mail: sachiko.s@gmail.com

*** Department of Mechanical Engineering, University of Nevada, Las Vegas
4505 Maryland Parkway, Las Vegas, NV, 89154-4015, USA

Abstract

In this study, acceleration responses of layered cylindrical structures are obtained using finite element analysis (FEA) and wave tracing technique. The wave tracing technique implies a direct application of the wave propagation equation which includes propagating wave and its reflections at the interfaces due to effect of impedance differences in layered structure. Wave tracing clearly supported FEA results which had showed that interference between applied impact and reflected waves affects wave propagation both negatively and positively depending on material combinations of the structure. The study showed that structures made in order of high-low-high impedance materials reduce magnitude of acceleration responses compared to homogeneous structures made of only high impedance material when there is no interference. While structures made in the order of low-high-low impedance materials reduce magnitude of acceleration responses compared to homogeneous structures made of only low impedance material with and without the interference. Furthermore, FEA results showed that structures made of high-low-high impedance materials reduce high frequency accelerations compared to homogeneous high impedance material structures. These results were experimentally verified with the previously reported results.

Key words: Impact, Mitigation, Reflection and Transmission Coefficients, Impedance, FEA and Layered Cylindrical Structure

1. Introduction

Smart projectiles have electronic devices to guide, navigate and control trajectories. Increasing accuracy and effectiveness of trajectories in smart projectiles has been critical in artillery science. However, failure of electronic devices in smart projectiles caused by high frequency and high accelerations induced during muzzle exit has often been observed. As mentioned by Refs. (1) and (2), a key component of a smart projectile must withstand high-g loads during launch. In general, electronic devices in a smart projectile must be small, economical and sustainable under high-g loading. In order to increase the impact tolerance of the electronic devices, the current accepted methods generally use a combination of stiffening and damping elements⁽³⁾. However, as Ref. (4) pointed out, the methods can not protect the electronic devices from high frequency accelerations which typically contain resonant frequencies of the sensitive internal components. Therefore, it is important to find new passive and effective ways to reduce high frequency vibrations in

*Received 28 May, 2010 (No. 10-0227)
[DOI: 10.1299/jmmp.4.1480]

Copyright © 2010 by JSME

Report Documentation Page				Form Approved OMB No. 0704-0188	
Public reporting burden for the collection of information is estimated to average 1 hour per response, including the time for reviewing instructions, searching existing data sources, gathering and maintaining the data needed, and completing and reviewing the collection of information. Send comments regarding this burden estimate or any other aspect of this collection of information, including suggestions for reducing this burden, to Washington Headquarters Services, Directorate for Information Operations and Reports, 1215 Jefferson Davis Highway, Suite 1204, Arlington VA 22202-4302. Respondents should be aware that notwithstanding any other provision of law, no person shall be subject to a penalty for failing to comply with a collection of information if it does not display a currently valid OMB control number.					
1. REPORT DATE MAY 2010		2. REPORT TYPE		3. DATES COVERED 00-00-2010 to 00-00-2010	
4. TITLE AND SUBTITLE Wave Propagation in Layered Cylindrical Structures Using Finite Element and Wave Tracing Analysis				5a. CONTRACT NUMBER	
				5b. GRANT NUMBER	
				5c. PROGRAM ELEMENT NUMBER	
6. AUTHOR(S)				5d. PROJECT NUMBER	
				5e. TASK NUMBER	
				5f. WORK UNIT NUMBER	
7. PERFORMING ORGANIZATION NAME(S) AND ADDRESS(ES) University of Nevada, Los Vegas, Department of Civil and Environmental Engineering, 4505 Maryland Parkway, Las Vegas, NV, 89154-4015				8. PERFORMING ORGANIZATION REPORT NUMBER	
9. SPONSORING/MONITORING AGENCY NAME(S) AND ADDRESS(ES)				10. SPONSOR/MONITOR'S ACRONYM(S)	
				11. SPONSOR/MONITOR'S REPORT NUMBER(S)	
12. DISTRIBUTION/AVAILABILITY STATEMENT Approved for public release; distribution unlimited					
13. SUPPLEMENTARY NOTES					
14. ABSTRACT					
15. SUBJECT TERMS					
16. SECURITY CLASSIFICATION OF:			17. LIMITATION OF ABSTRACT Same as Report (SAR)	18. NUMBER OF PAGES 16	19a. NAME OF RESPONSIBLE PERSON
a. REPORT unclassified	b. ABSTRACT unclassified	c. THIS PAGE unclassified			

projectiles in order to protect their electronic devices.

Previously, Ref. (5) showed analytically that the amplitude of a wave is reduced at the interface of a layered composite material when the material of lower impedance is placed before the material of higher impedance. Similarly, Ref. (6) reported that the propagating wave attenuates over certain frequency bands due to the periodic stiffness discontinuities in a relatively long shell. By periodically adding rings around a shell, the impedance changes occur as a result of the induced periodic discontinuities in its stiffness. They pointed out that it is possible to obtain the desired attenuation of wave propagation by periodically adjusting the impedance. Recently, Ref. (7) studied mitigation of high frequency vibrations in a projectile using wave speed mismatch. They concluded that attenuation of acceleration at the end of a projectile occurs when a shock wave crosses from high to low and back to high wave speed mediums, which differs slightly from the conclusion drawn by Ref. (5). The attenuation phenomena may be explained based on the wave reflection and transmission at the boundaries. However, our studies show that the phenomenon does not have a straight forward explanation. The studies suggest that interference between an applied impact and propagating waves might impede the attenuation of the wave depending on the time interval and the travel time of the reflected wave. Therefore, in this paper, wave propagations in layered cylindrical structures are studied using FEA and the results are compared with the basic equations of wave propagation in layered media. Also, FEA results are experimentally verified using previously reported results and discussed in the result section.

2. Research Method

2.1 Structural configuration

Solid cylindrical structures with overall length of 203.2 mm and 101.6 mm diameter are used to study the axial direction of wave propagations. Six different configurations (Fig. 1) are used for two main objectives. The first objective is to study how acceleration response changes depending on material or material combinations. Four structural configurations are compared which are made of (1) all aluminum, (2) all polycarbonate, (3) aluminum at two ends and polycarbonate at the middle, and (4) polycarbonate at two ends and aluminum at the middle. These configurations are namely; (1) Al, (2) Poly, (3) APA-2, and (4) PAP. Each end plate has 50.8 mm length and the middle plate has 101.6 mm length for both “APA-2” and “PAP” configurations. The second objective is to study effect of various material lengths. Here, three different layer conditions are used; (i) 25.4 mm aluminum followed by 101.6 mm

mm polycarbonate and 76.2 mm aluminum, (ii) 50.8 mm aluminum, 101.6 mm polycarbonate and 50.8 mm aluminum, and (iii) 76.2 mm aluminum, 101.6 mm polycarbonate and 25.4 mm aluminum. These configurations, (i), (ii) and (iii) are called “APA-1”, “APA-2” and “APA-3”, respectively. The first layer of structures is referred to the impact side. For instance, an impact is

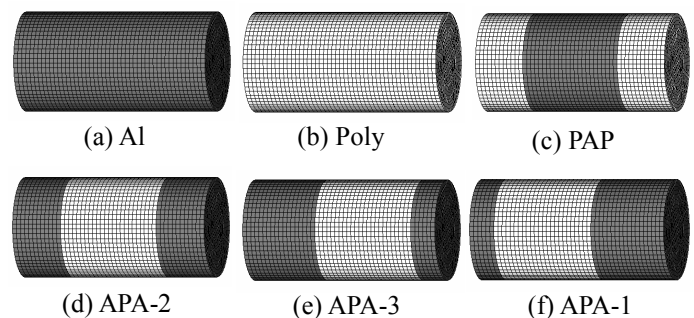


Figure 1. Six different configurations used in the study. Overall size of each structure is the same (203.2 mm length with 101.6 mm diameter). Dark and light colors represent aluminum and polycarbonate parts, respectively. An impact is applied at the left end of cylindrical structures made of (a) aluminum only, (b) polycarbonate only, (c) 50.8 mm polycarbonate, 101.6 mm aluminum and 50.8 mm polycarbonate, (d) 50.8 mm aluminum, 101.6 mm polycarbonate and 50.8 mm aluminum, (e) 76.2 mm aluminum, 101.6 mm polycarbonate and 25.4 mm aluminum, and (f) 25.4 mm aluminum, 101.6 mm polycarbonate and 76.2 mm aluminum.

applied to layer of 25.4 mm aluminum when “APA-1” structure is used.

2.2 Finite Element Analysis

Acceleration responses at the center node at the end of cylindrical structures are computed under impact load using the finite element software, LS-DYNA⁽⁸⁾. The cylindrical structure is modeled using 23,424 elements (eight-node solid hexahedron) with the aid of

Altair HyperMesh software⁽⁹⁾. In the computational process, one-point Gaussian quadrature is used to carry out the volume integration and constant stress solid element type is chosen to save computational time^{(10) and (11)}. An impact load is applied at the nine center nodes of the cylindrical structure as a half sine curve. In this study, two different half sine curves are used to apply impacts; low magnitude with long period (Force 1) and high magnitude with short period (Force 2). Both curves have the same impulse as shown in Fig. 2. Materials used in the structures, aluminum and polycarbonate, are defined using *MAT_PLASTIC_KINEMATIC in LS-DYNA models excluding strain-rate effects. Material properties used in the computational study are tabulated in Table 1. When two different materials are used in the structure, nodes between two materials are shared in the finite element model and there is no contact surface or elements defined between materials.

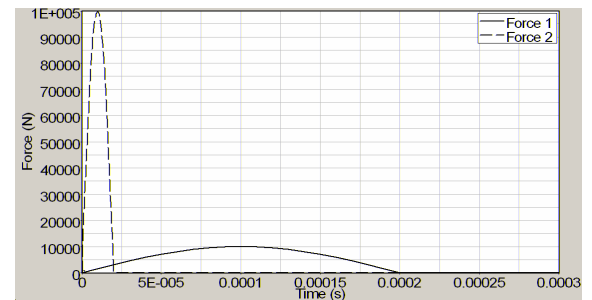


Figure 2. Two impact forces of equal impulses used in the computational study. Force 1 has magnitude of 10,000 N with impact duration of 0.2×10^{-3} seconds and Force 2 has magnitude of 100,000 N with impact duration of 0.02×10^{-3} seconds.

2.3 Wave Propagation

Since acceleration at the face of the cylindrical structure is of interest, vibration traveling along the cylindrical structure is treated as longitudinal wave propagation in a rod. The equation of motion of longitudinal wave propagation can be expressed by Eq. 1 assuming that plane transverse sections of the cylindrical structure remain plane during the passage of the wave, thus no shear wave effect.

$$\rho \frac{\partial^2 u}{\partial t^2} = E \frac{\partial^2 u}{\partial x^2} \quad \text{Equation 1}$$

Where, ρ and E are the material density and Young's modulus, respectively. u is the displacement in x direction and t represents time. The wave propagates in the structure with the speed of $\sqrt{E/\rho}$. In order for Eq. 1 to be valid, the assumption must be such that no transverse or shear waves are generated, and the impulse generated waves travel axially. At the same time transverse and shear waves are negligible due to concentricity and to the axial nature of the impact force and its short duration. Meanwhile, if the wave encounters an interface, the part of the wave reflects back and the rest passes through the interface. If a wave with amplitude $a(t)$ in medium 1 encounters a boundary with medium 2, the amplitudes of the reflected, a_r , and transmitted, a_t , waves are determined by following equations.

$$a_r = \frac{Z_2 - Z_1}{Z_1 + Z_2} a(t) \quad \text{Equation 2}$$

Table 1. Material properties of aluminum and polycarbonate

	Density	Young's Modulus	Poisson's Ratio	Yield Strength	Wave Speed	Impedance
	ρ (Kg/m ³)	E (GPa)	μ	σ_y (MPa)	c (m/s)	Z
Aluminum	2700.0	70.00	0.33	250.00	5091.8	1.37E+07
Polycarbonate	1200.0	2.30	0.35	62.00	1384.4	1.66E+06

$$a_i = \frac{2Z_2}{Z_1 + Z_2} a(t) \quad \text{Equation 3}$$

Where, Z_1 and Z_2 are the characteristic impedances of material 1 and 2, obtained by multiplying its material density and wave speed. The equations, however, to be varied, the applied force should not interfere with the propagating wave.

In the case of undamped spring-mass system, the motion under a half-sine pulse excitation (Eq. 4) is expressed as a second order differential equation, Eq. 5⁽¹²⁾.

$$\begin{aligned} F(t) &= F_0 \sin \frac{\pi t}{t_1} & \text{for } t < t_1 \\ &= 0 & \text{for } t > t_1 \end{aligned} \quad \text{Equation 4}$$

$$\begin{aligned} \ddot{x} + \omega_n^2 x &= \frac{F_0}{m} \sin \frac{\pi t}{t_1} & \text{for } t < t_1 \\ &= 0 & \text{for } t > t_1 \end{aligned} \quad \text{Equation 5}$$

The solution of the equation with the initial conditions $x(0) = \dot{x}(0) = 0$ is

$$\begin{aligned} \frac{xk}{F_0} &= \frac{1}{\frac{\tau}{2t_1} - \frac{2t_1}{\tau}} \left[\sin \frac{2\pi t}{\tau} - \left(\frac{2t_1}{\tau} \right) \sin \frac{\pi t}{t_1} \right] & \text{for } t < t_1 \\ &= \frac{1}{\frac{\tau}{2t_1} - \frac{2t_1}{\tau}} \left[\sin \frac{2\pi t}{\tau} + \sin \left(\frac{t}{\tau} - \frac{t_1}{\tau} \right) \right] & \text{for } t > t_1 \end{aligned} \quad \text{Equation 6}$$

$$\begin{aligned} \ddot{x} &= \frac{4F_0\pi^2 \left(-2t_1 \sin \frac{2\pi t}{\tau} + \tau \sin \frac{\pi t}{t_1} \right)}{\tau k (\tau^2 - 4t_1^2)} & \text{for } t < t_1 \\ &= \frac{8F_0t_1\pi^2 \left(-\sin \frac{2\pi t}{\tau} + \sin \frac{2\pi(-t+t_1)}{\tau} \right)}{\tau k (\tau^2 - 4t_1^2)} & \text{for } t > t_1 \end{aligned} \quad \text{Equation 7}$$

where, x is deformation, ω_n and τ are the natural frequency and period, F_0 and t_1 are the maximum force and impact duration of the excitation pulse and m is the mass of the system. The stiffness of the system, k is calculated by following equation;

$$k = \sqrt{\frac{AE}{L}} \quad \text{Equation 8}$$

where, A and L are the circular area and length of the cylindrical structure, respectively, and E is the Young's modulus. Acceleration of the system (Eq. 7) is obtained by differentiating Eq. 6 twice.

3. Computational Results

3.1 Effect of material combinations

Figure 3 shows acceleration responses computed at the end of four different configurations of the cylindrical structures shown in Fig. 1. Impact force of magnitude of 10,000 N and 0.2×10^{-3} seconds impact duration were applied to the cylindrical structures (Force 1 in Fig. 2). Four different material combinations are "Al", "Poly", "APA-2" and "PAP". The highest magnitude of acceleration response, $90,172 \text{ m/s}^2$, was observed in "Poly" followed by "PAP" ($66,647 \text{ m/s}^2$). The other two configurations, "Al" and "APA-2", had $8,898$ and $8,727 \text{ m/s}^2$ maximum accelerations which were approximately ten times lower than the acceleration response of "Poly" and "PAP" shown in Fig. 3. Important difference between the acceleration responses of "Al" and "APA-2" was that high frequencies in "APA-2" was significantly reduced which helps to prevent damages in

electronic devices.

Figure 4 shows acceleration responses obtained using the same configurations as Fig. 3. However, the applied impact is ten times higher in magnitude (100,000 N) with ten times shorter impact duration (0.02×10^{-3} seconds) having the same impulse as the first impact, Force 1. The force is shown as Force 2 in Fig. 2. The order of maximum acceleration was same as the one obtained using Force 1. However, the noticeable difference between the two impact forces was observed in the maximum accelerations. When Force 2 was used, “Poly” had the highest maximum acceleration of approximately $2.38 \times 10^6 \text{ m/s}^2$ while “PAP” and “Al” had approximately twice lower than that of “Poly” (approximately $1.17 \times 10^6 \text{ m/s}^2$ for “PAP” and $1.05 \times 10^6 \text{ m/s}^2$ for “Al”). Maximum acceleration in “APA-2” was about $0.48 \times 10^6 \text{ m/s}^2$, which was approximately five times lower than that of “Poly”. It is also important to note that the peak frequencies in “APA-2” showed much faster attenuation of higher frequencies and acceleration magnitudes compared to other configurations. This is an important factor in reducing damages to electronic devices since high frequency accelerations contain resonant frequencies of sensitive components.

Differences in acceleration response depending on impact forces observed in FEA results match with previously reported experimental results⁽¹³⁾. The experiments were conducted using two structures, namely “Al-Al-Al” and “Al-Nylon-Al”. Both structures have overall length of 2.26 m and 25 mm diameter and are made of either aluminum or aluminum and nylon similar to the FEA simulation structures, “Al” and “APA-2”, respectively. Two different forces with the same impulse were applied using an impulse hammer to compare the acceleration responses at the end of the suspended cylindrical structure. As shown in Fig. 5, when the impact with long duration was applied, maximum accelerations were similar for both structures. However, when a shorter impact duration was used, maximum acceleration is significantly reduced. The agreement in FEA and experimental results confirm that the results obtained from FEA are verified.

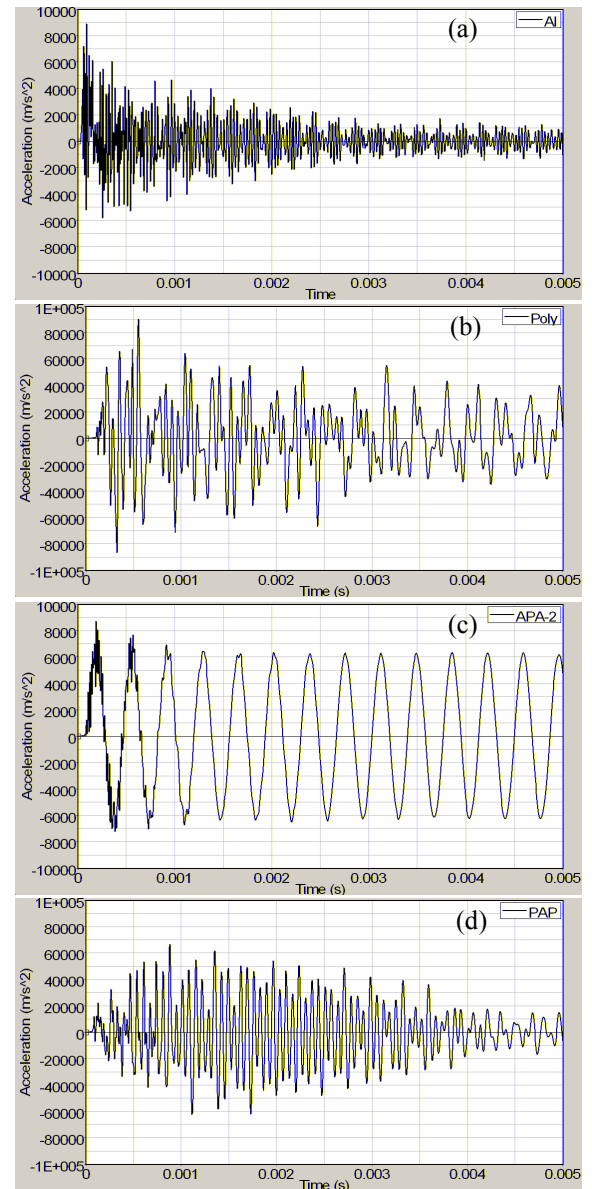


Figure 3. Acceleration responses of four different cylindrical configurations using a half-sine impact force magnitude of 10,000 N with impact duration of 0.2×10^{-3} seconds. The four acceleration plots are obtained using cylindrical structures made of (a) aluminum, (b) polycarbonate, (c) aluminum ends with polycarbonate at the middle and (d) polycarbonate ends with aluminum at the middle.

3.2 Effect of material length

Material order, aluminum, polycarbonate and aluminum, are used to study acceleration changes based on the material length. Three configurations, “APA-1”, “APA-2” and “APA-3” are used to compare acceleration responses. When Force 1 (10,000 N with 0.2×10^{-3} seconds impact duration) was used, accelerations in all three configurations are similar to each other as shown in Fig. 6. Maximum accelerations of “APA-1”, “APA-2” and “APA-3” are 7,629, 8,727, and 7,464 m/s^2 , respectively. When Force 2 which is a higher magnitude and a shorter impact duration than Force 1, was applied to the three cylindrical configurations, differences in maximum accelerations were more pronounced. The highest maximum acceleration was observed in “APA-2” ($\approx 478,980 \text{ m/s}^2$). The other two configurations had maximum accelerations of 196,540 m/s^2 for “APA-1” and 220,960 m/s^2 for “APA-3”, showing an acceleration mitigation of more than 50 % and a much faster attenuation of accelerations.

4. Results from wave propagation

4.1 Wave Tracing

Simple calculations are carried out using the basic theory described in the preceding section to relate the computational results with wave propagation phenomena. Material wave speeds and impedances of aluminum and polycarbonate were calculated based on the material properties shown in Table 1. The transmission and reflection coefficients from aluminum to polycarbonate layers are calculated as 0.22 and -0.78, respectively, using Eqs. 2 and 3. Similarly, coefficients from polycarbonate to aluminum are 1.78 for transmission and 0.78 for reflection. Coefficients applied to each layer condition are shown in Fig. 8.

Wave propagations in six different configurations with two impact force conditions are traced using the coefficients shown above and results are shown in Figs. 9 to 13. Only selected results are presented here due to space limitations. The horizontal direction in the figures shows the length of cylindrical structure and vertical direction shows time. A wave starts propagating as the impact is applied on the left side of the structure, and propagating

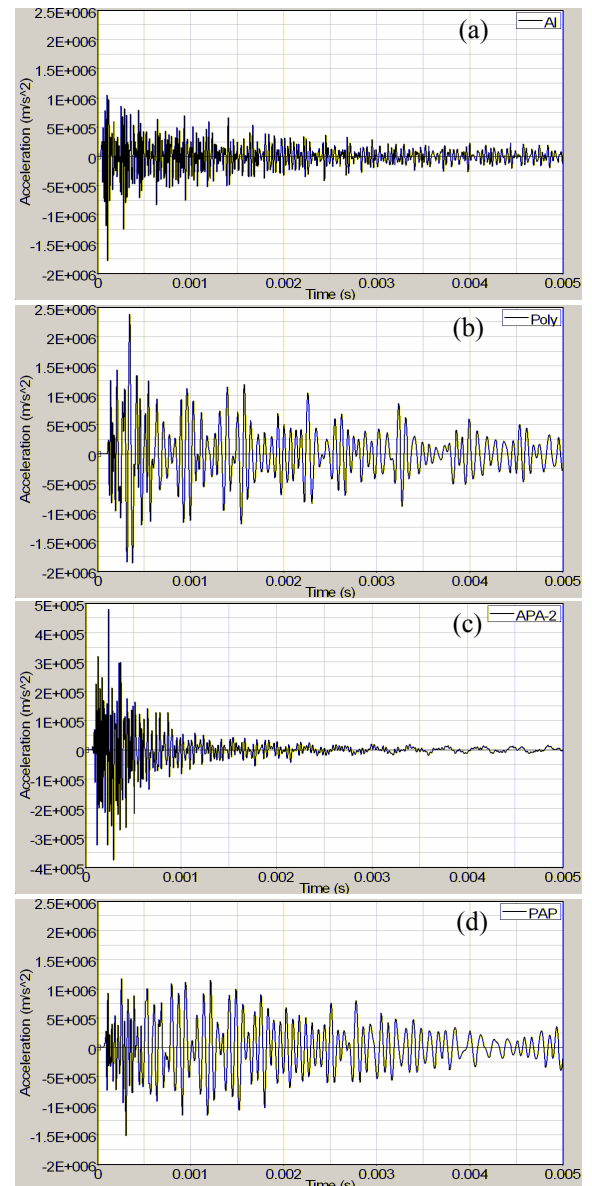


Figure 4. Acceleration responses of four different cylindrical configurations using a half-sine impact force magnitude of 100,000 N with impact duration of 0.02×10^{-3} seconds. The four acceleration plots are obtained using cylindrical structures made of (a) aluminum, (b) polycarbonate, (c) aluminum ends with polycarbonate at the middle and (d) polycarbonate ends with aluminum at the middle.

waves are shown as lines in the horizontal direction. The numbers in the figures represent transmitted, reflected or combination of both waves calculated based on the applied impact shown in the left side of figures. Positive values indicate compressive wave and negative tensile. For instance, Fig. 10 shows the wave tracing of “APA-2”. When 1.56×10^3 N force is applied at the left side of the structure at 0.01 ms, the wave starts propagating through the first aluminum layer and encounters the interface between aluminum and polycarbonate layers. At this point, 22% of propagating wave (0.34×10^3 N) transmits to the second polycarbonate layer and -78% (-1.22×10^3 N) reflects back into the first aluminum layer.

Transmitted and reflected waves continue while interfering with each other or with applied impact forces.

Same as computational study, two half-sine forces, Force 1 and Force 2, are considered, Force 1 as 10,000 N maximum magnitude with impact duration of 0.2×10^{-3} seconds and Force 2 as 100,000 N maximum magnitude with impact duration of 0.02×10^{-3} seconds.

4.1.1 Effect of material combinations

Figure 9 shows “Al” and “Poly” cases under the action of Force 1. Since waves can propagate much faster in aluminum than in polycarbonate, the propagating waves return to the initiation point (at the point of impact) after about 0.08×10^{-3} seconds over a total length of eight inches and start to interfere with the applied impact. For the “Poly” case, waves return to the original point after about 0.2×10^{-3} seconds. Therefore the impact will be over by the time a wave reflects back to the impact point, thus there will be no interference. As a result, “Al” experienced the maximum wave amplitude of 16.18×10^3 N which is larger than the maximum magnitude of applied impact, 10.0×10^3 N, while “Poly” showed the maximum wave amplitude of 10.0×10^3 N. Fig. 10 shows wave tracing of “APA-2” under the action of Force 1. In this case, a propagating wave started reflecting back immediately to the starting point when the wave reached the first interface between aluminum and polycarbonate layers. Since the first aluminum layer is much shorter than the “Al” case, the wave reflects back quickly. As a result, interference between the applied impact and reflected back wave starts early. The reflection coefficient at the interface between aluminum and polycarbonate has a negative sign (polarity changes after reflection). However the reflection coefficient at the free ends also has a negative sign. Therefore, the applied impact and reflected wave have the same polarity resulting in addition of their amplitudes. Even though the reflected and transmitted waves at the interfaces have lower magnitudes than the original wave, in this case between the reflected wave and the impact wave interference increases magnitude of the wave. Consequently, the maximum wave reaching the right end significantly increased to 43.34×10^3 N. On the other hand, when “PAP” was used with a half-sine curve impact, the maximum wave reaching to the right end

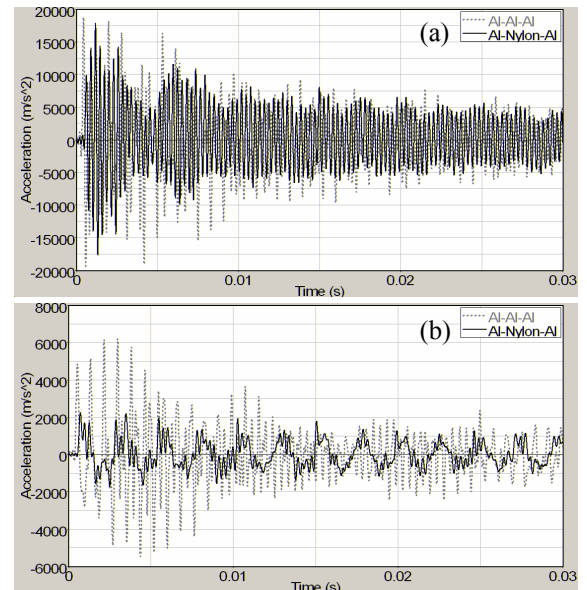


Figure 5. Experimental results reported in Ref. (13). Acceleration responses are obtained using (a) long impact duration and (b) short impact duration. 5,000 Hz cutoff frequency is used for low-pass filter. Al-Al-Al represents structure made of aluminum and Al-Nylon-Al is made of aluminum and nylon.

decreased to 5.46×10^3 N (Fig. 11). When a polycarbonate layer comes first, reflected wave at the first interference has the same sign as the incident wave. Therefore, when interferences started between applied impact and reflected wave at the free end, impact and the reflected wave have opposite signs which results in reduction of magnitude of propagating wave.

Wave tracing are also obtained using Force 2 (100,000 N with 0.02×10^{-3} seconds impact duration). Since the impact is applied with much shorter period than that of Force 1, there is no interference between reflected wave and applied impact. Therefore, changes in propagating wave occurs only at the interfaces resulting in slight reduction in the maximum magnitude of the waves reaching the right end of “APA-2” (Fig. 12) and “PAP” (not shown here). There are no magnitude changes in propagating wave of “Al” and “Poly” since there are no interfaces in those two configurations. The maximum magnitude of wave for “APA-2” was 89.34×10^3 N and for “PAP” was 97.00×10^3 N.

4.1.2 Effect of material length

Wave tracing of “APA-1” and “APA-3” are also studied under two impact forces (Force 1 and 2). Wave tracing figures are not shown here except “APA-1” with Force 1. Since the first layer of “APA-1” is shorter than that of “APA-3”, the interference between applied impact and reflected wave in “APA-1” starts slightly earlier than in “APA-3”. As mentioned earlier, when the reflected wave interferes with an applied impact in the order of aluminum and polycarbonate, two waves show constructive interference and increase magnitude of propagation. Therefore, increasing interference resulted in slightly higher maximum magnitude of wave in “APA-1” (43.21×10^3 N) compared to “APA-3” (43.03×10^3 N). On the other hand, when Force 2 (shorter impact duration) was applied, “APA-1” showed lower maximum magnitude of wave than that of “APA-3”. The maximum magnitude of waves in “APA-1” and “APA-3” were 49.13×10^3 N and 54.42×10^3 N, respectively. When wave transmits from polycarbonate to aluminum layer, magnitude of wave increases significantly because of the transmission coefficient. Therefore, it is better to have smaller magnitude of transmitted waves from polycarbonate to aluminum layer in order to reduce waves. On the other hand, longer third layer helps to reduce the reflected wave at the end of the cylinder which interferes with the transmitted wave from polycarbonate to aluminum, causing an increase in the propagating waves by adding up two waves. Since “APA-3” has shorter third

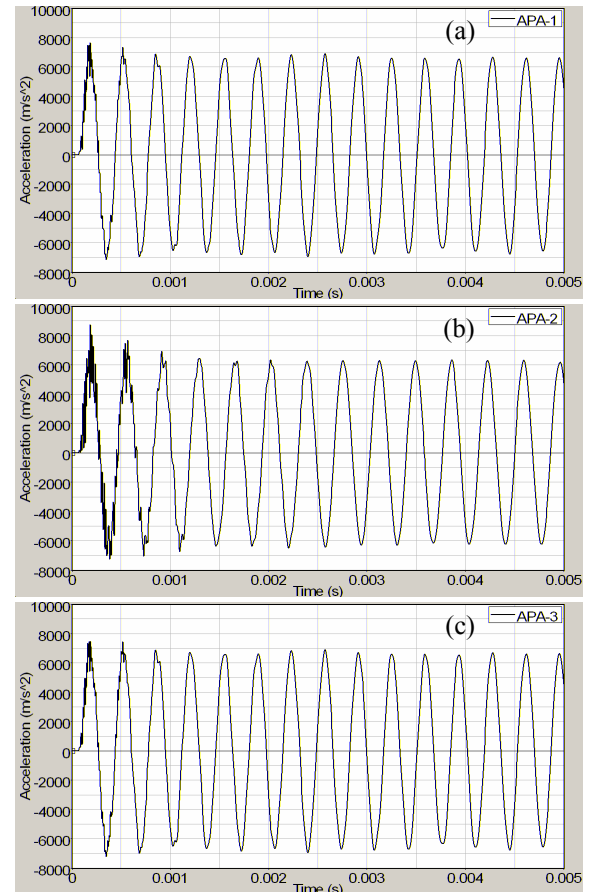


Figure 6. Acceleration responses obtained applying a half-sine impact of 10,000 N with 0.2×10^{-3} seconds impact duration. The three acceleration plots are obtained using the layered structure made of (a) 25.4 mm aluminum, 101.6 mm polycarbonate and 76.2 mm aluminum, (b) 50.8 mm aluminum, 101.6 mm polycarbonate and 50.8 mm aluminum, and (c) 25.4 mm aluminum, 101.6 mm polycarbonate and 76.2 mm aluminum.

layer than “APA-1”, “APA-3” has more propagating waves in the third layer because of increase in reflections. As a result, “APA-3” increases the maximum wave.

When “APA-2” was used, the maximum magnitude of wave reached to the end was much higher than that of “APA-1” and “APA-3” when there is no interference between the applied impact and reflected wave. This is caused by the interference between reflected and transmitted waves at the interfaces. At both interfaces (between layers one and two, and two and three), “APA-2” always interfere with other reflected or transmitted waves since waves reach at the same time. However, propagating waves in “APA-1” and “APA-3” do not always interfere with each other because of the differences in material length causing changes in propagation time. Therefore, “APA-2” has apparently higher maximum magnitude of wave. Similarly, when there was interference between the applied impact and reflected wave, “APA-2” showed higher maximum magnitude of wave although not as high as in the case without interference.

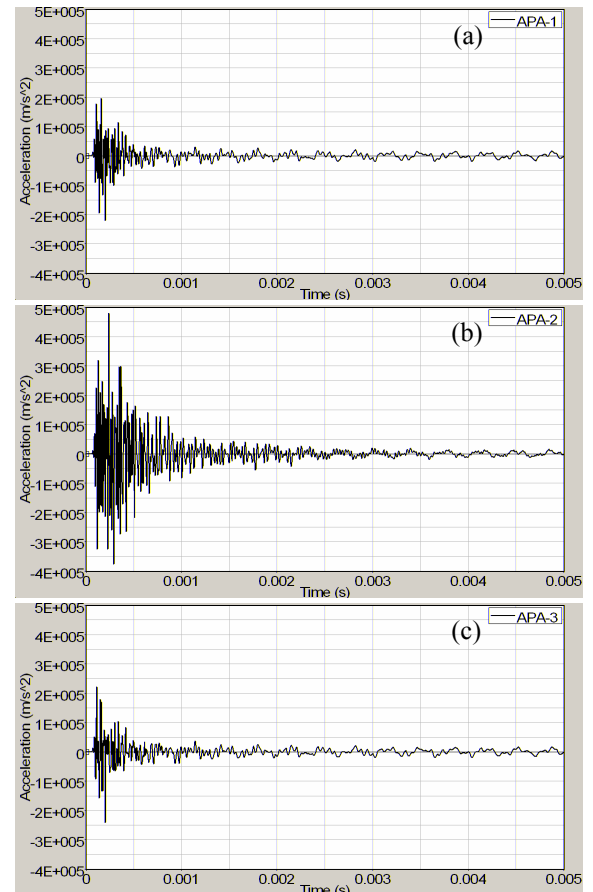


Figure 7. Acceleration responses obtained applying a half-sine impact of 100,000 N with 0.02×10^{-3} seconds impact duration. The three acceleration plots are obtained using the layered structure mode of (a) 25.4 mm aluminum, 101.6 mm polycarbonate and 76.2 mm aluminum, (b) 50.8 mm aluminum, 101.6 mm polycarbonate and 50.8 mm aluminum, and (c) 25.4 mm aluminum, 101.6 mm polycarbonate and 76.2 mm aluminum.

4.2 Acceleration from equation of motion for undamped spring-mass system

Accelerations in the cylindrical structures under a half-sine curve impulse can be calculated using the equation shown above (Eq. 7). When a half-sine force of 10,000 N at the peak with 0.2×10^{-3} seconds impact duration (Force 1) was applied to “Al” and “Poly”, Eq. 7 can be written by substituting the material properties shown in Table 1 as,

$$\text{Al: } \ddot{x} = 2322\sin(25058t) - 1455\sin(15708t) \quad \text{Equation 9}$$

$$\text{Poly: } \ddot{x} = -2702\sin(6813t) + 6231\sin(15708t) \quad \text{Equation 10}$$

From the above equations, the maximum acceleration in “Poly” was obtained as approximately $4,600 \text{ m/s}^2$, which was nearly twice as high as that of “Al” ($\approx 2,700 \text{ m/s}^2$). Similarly, when a half-sine force of 100,000 N at the peak with 0.02×10^{-3} seconds impact duration (Force 2) was applied, Eq. 7 can be written for “Al” and “Poly” as

$$\text{Al: } \ddot{x} = -3680\sin(25058t) + 23069\sin(15708t) \quad \text{Equation 11}$$

$$\text{Poly: } \ddot{x} = -2198\sin(6813t) + 50680\sin(15708t) \quad \text{Equation 12}$$

From the above equation, the difference in the maximum acceleration was slightly higher than the result obtained using Force 1. The maximum acceleration in “Poly” was about $51,000 \text{ m/s}^2$, while in “Al” it was approximately $22,000 \text{ m/s}^2$. The differences in the

acceleration response in the “Al” and “Poly” are due to the differences in their mass densities and Young’s moduli.

5. Discussions

Computational results showed that “APA-2” has the lowest maximum acceleration among four different configurations; “Al”, “Poly”, “PAP” and “APA-2” whether the impact duration is long (0.2×10^{-3} seconds) or short (0.02×10^{-3} seconds). However, this was not the case when waves were traced using reflected and transmitted equations (Eqs. 2 and 3). When the wave was traced, the order of maximum magnitude of wave reached at the end of

the cylindrical structures changed depending on the impact duration. When the impact with long impact duration (0.2×10^{-3} seconds) was used, the highest magnitude of waves were observed in “APA-2”, followed by “Al”, “Poly” and “PAP”. On the other hand, when the impact was applied with shorter impact duration (0.02×10^{-3} seconds), the highest magnitude of wave was in “Al” and “Poly” followed by “PAP”, and the lowest maximum wave was in “APA-2”. This difference may be caused by excluding effect between applied impact and acceleration response based on material. When the equation of motion was used to calculate the acceleration response, the acceleration showed significant differences between aluminum and polycarbonate. Polycarbonate has much higher magnitude of acceleration response than that of aluminum under the same impact condition. For instance, the wave tracing showed 16.18×10^3 N maximum magnitude in “Al” and 10.00×10^3 N in “Poly”, concluding that “Al” has higher maximum magnitude of wave. However, acceleration from the motion of equation showed approximately twice as much acceleration in “Poly” than “Al”. Therefore, the combined force results obtained from wave tracing and accelerations from the equation of motion for “Poly” ended up having higher maximum acceleration. It is clear that when different materials were used at the impact face, wave tracing might not be useful to study magnitude of wave propagation phenomena. However, the wave tracing clearly showed the differences within the same material combinations. When the material order of aluminum, polycarbonate and aluminum was used with short impact duration force, the wave tracing results showed that the number of interference incidences between reflected and transmitted waves is higher in “APA-2” resulting in increased maximum magnitude compared to “APA-1” and “APA-3”. On the other hand, when there is interference between the applied impact and the reflected wave, the interference increases the maximum wave amplitude significantly and the reductions at the material interfaces become almost negligible.

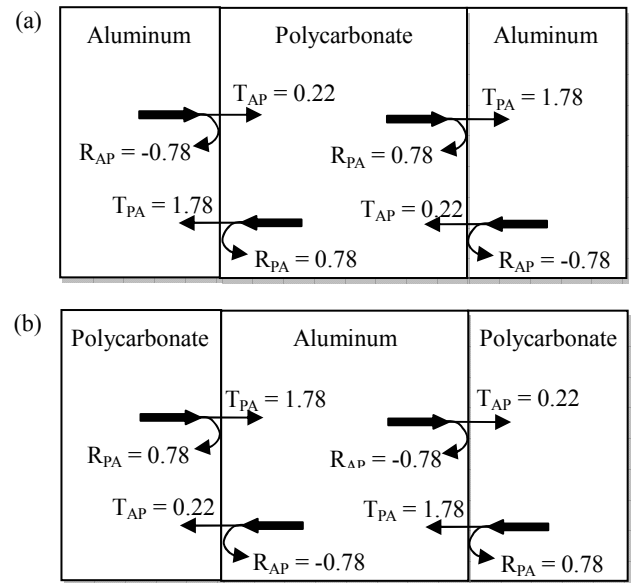


Figure 8. Transmission and reflection coefficients for (a) aluminum-polycarbonate-aluminum and (b) polycarbonate-aluminum-polycarbonate layer configurations. T_{AP} and T_{PA} represents transmission coefficient from aluminum to polycarbonate and polycarbonate to aluminum, respectively. Similarly, R_{AP} represents reflection coefficient of wave which propagates aluminum layer and reflects at the interface between aluminum and polycarbonate and R_{PA} is reflection coefficient of the opposite layer condition.

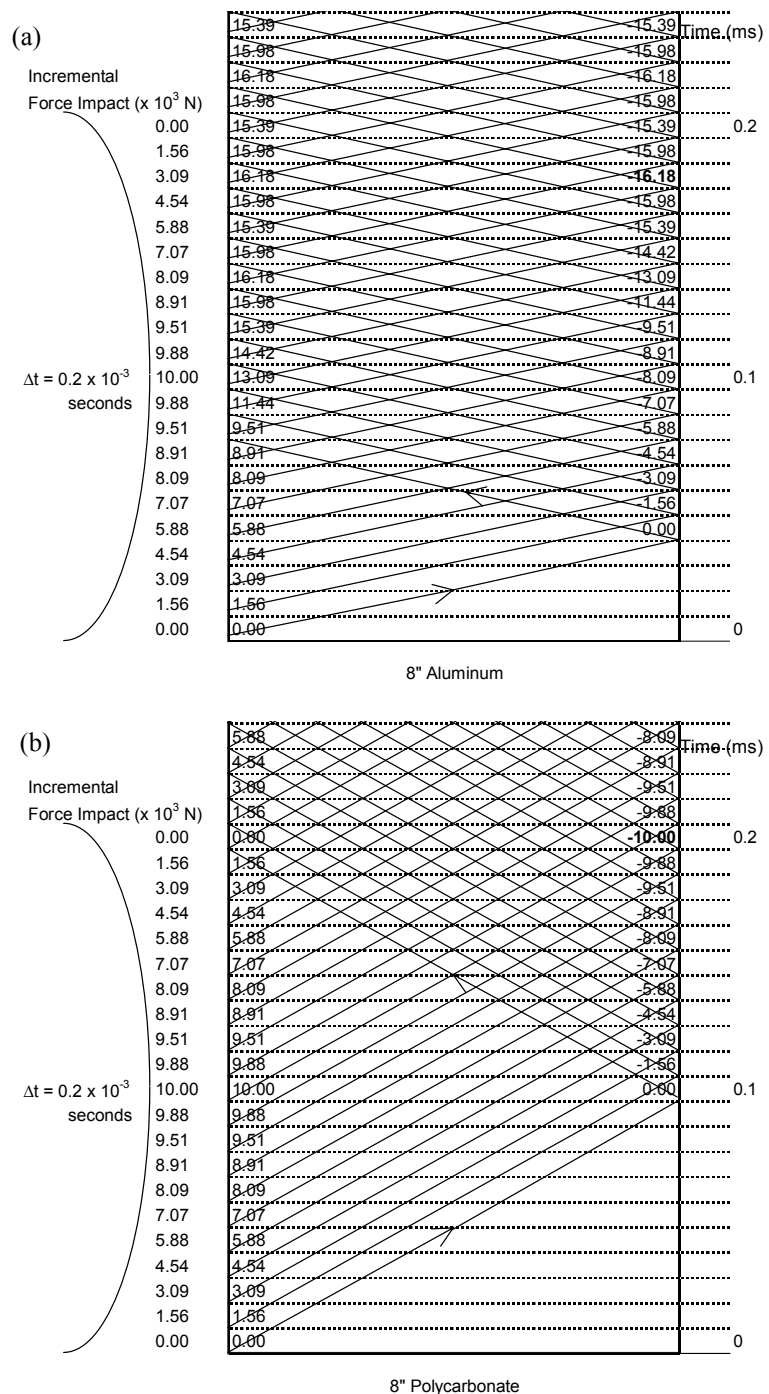


Figure 9. Wave tracing of (a) “Al” and (b) “Poly” under a half-sine impact with a maximum magnitude of 10×10^3 N and an impact duration of 0.2×10^{-3} seconds. Maximum propagated wave at the right end is 16.18×10^3 N. Column values represent the magnitude of the propagating wave in kN. Positive values indicate a compressive wave and negative tensile.

Wave tracing also showed when “PAP” is used, a reflected wave from the first interface reduces magnitude of propagating wave by interfering with the applied impact. However, acceleration magnitude significantly changes depending on materials used in a structure based on their densities and Young’s modulus. As shown in the results obtained from the FEA and the equation of motion, “Poly” had much higher magnitude of acceleration than that of “Al” under the same applied impact force. Therefore, when the acceleration response of “PAP” is compared with that of “Al”, since “Al” has higher density and Young’s

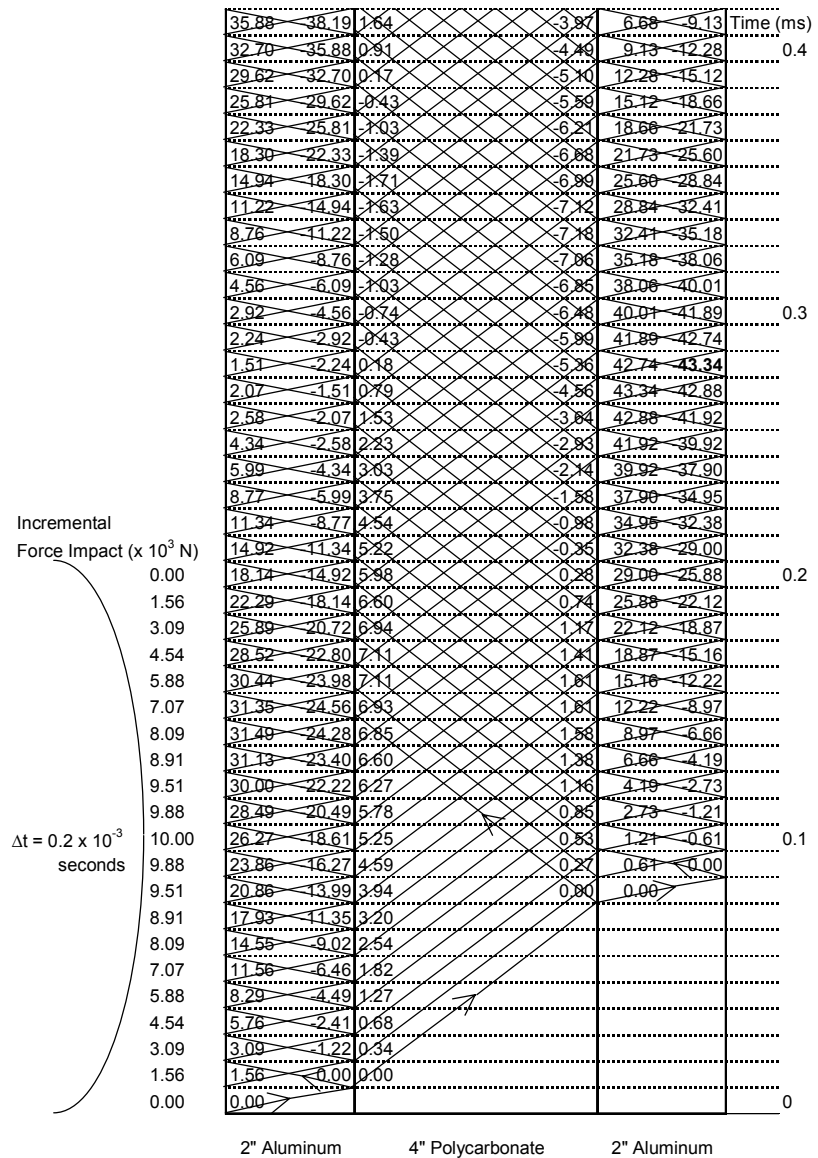


Figure 10. Wave tracing of “APA-2” under a half sine impact with a maximum magnitude of 10×10^3 N and an impact duration of 0.2×10^{-3} seconds. Maximum propagated wave at the right end is 43.34×10^3 N. Column values represent the magnitude of the propagating wave in kN. Positive values indicate a compressive wave and negative tensile.

modulus, “PAP” showed much higher magnitude of acceleration response. On the other hand, when “PAP” is compared with that of “Poly”, “PAP” showed lower magnitude of accelerations even though “Poly” has lower density and Young’s modulus. Therefore, in this case, the impedance mismatch seemed to affect the magnitude of accelerations more compared to the differences in their densities and Young’s modulus.

Unlike “Al” and “APA” cases where differences in the acceleration responses change depending on the interference between an applied impact and reflected wave, “PAP” always showed lower magnitude of accelerations compared to “Poly”. This is because the interference between an applied impact and reflected wave helps to reduce the magnitude of propagating wave in “PAP”.

6. Conclusions

Acceleration responses of layered cylindrical structures were studied computationally and discussed interference phenomenon and effect of material properties based on the wave

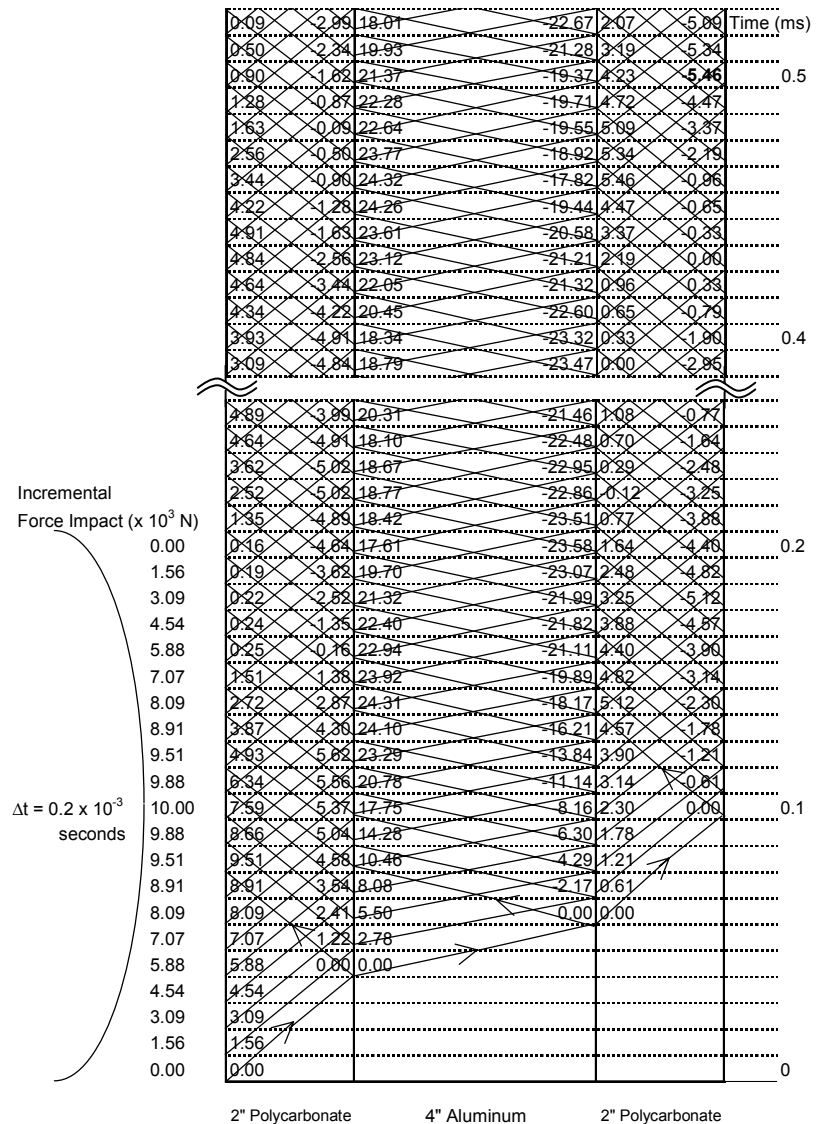


Figure 11. Wave tracing of “PAP” under a half sine impact with a maximum magnitude of 10×10^3 N and an impact duration of 0.2×10^{-3} seconds. Maximum propagated wave at the right end is 5.46×10^3 N. Column values represent the magnitude of the propagating wave in kN. Positive values indicate a compressive wave and negative tensile.

tracing and the equation of motion. The computationally obtained acceleration response showed that “APA-2” has the lowest maximum acceleration compared to “Al”, “Poly” and “PAP”. The acceleration of “Poly” was significantly higher than “Al” because of its material properties under the same impact force. The “PAP” also had much higher acceleration compared to “Al” and the layered structures from aluminum, polycarbonate and aluminum combination since the impact face is made of polycarbonate. However, polycarbonate, aluminum and polycarbonate combination helps to reduce impact force by interfering with reflected wave as explained by wave tracing. On the other hand, the combination of aluminum, polycarbonate and aluminum does not cause any change in magnitude of wave propagation when there is interference between the applied impact and the reflected wave. Therefore it is beneficial to use the combination of aluminum, polycarbonate and aluminum to attenuate wave propagation when applied impact is shorter or the structure is long enough such that there is no interference between the applied impact and reflected back wave. If the combination of polycarbonate, aluminum and polycarbonate is compared with the structure made of polycarbonate only, then the one with combination

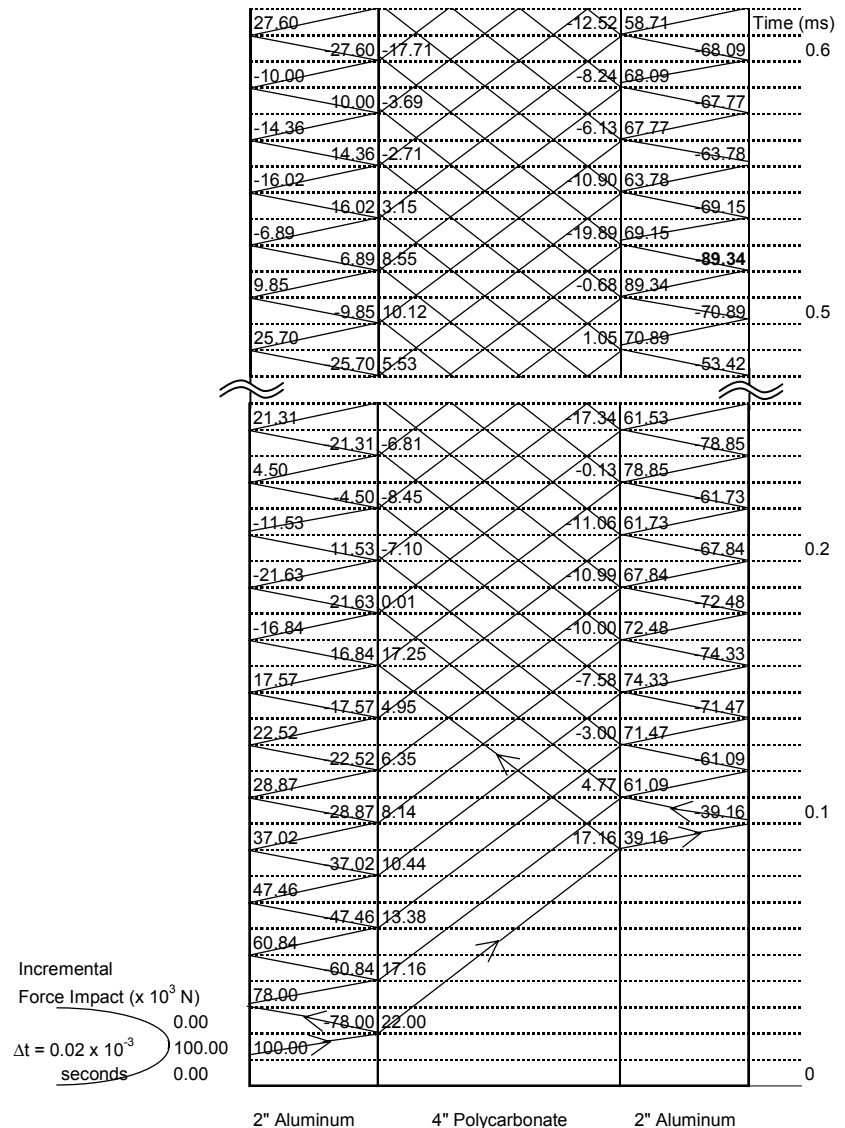


Figure 12. Wave tracing of “APA-2” under a half sine impact with a maximum magnitude of 100×10^3 N and an impact duration of 0.02×10^{-3} seconds. Maximum propagated wave at the right end is 89.34×10^3 N. Column values represent the magnitude of the propagating wave in kN. Positive values indicate a compressive wave and negative tensile.

helps to reduce the wave propagation without considering the interference.

In summary, interference between an applied impact and reflected wave is one of the important elements to consider in addition to magnitudes of wave propagation and material combinations. The combination of high-low-high impedance structure reduces magnitude of acceleration compared to only high impedance structure if there is no interference between applied impact and reflected waves while low-high-low impedance material structure reduces magnitude of acceleration with or without the interference. However, high-low-high impedance combination attenuates the higher frequency acceleration compared to high impedance material structure which was not the case when low-high-low impedance combination was compared with only low impedance structure.

Length of the materials also affects occurrence of interferences within the structure causing changes in magnitude of wave propagation, especially when there is no interference between applied impact and reflected waves. Wave tracing results clearly showed if there is fewer interferences within the structures under the same material combination (aluminum, polycarbonate and aluminum), maximum wave reached to the end of structure is reduced.

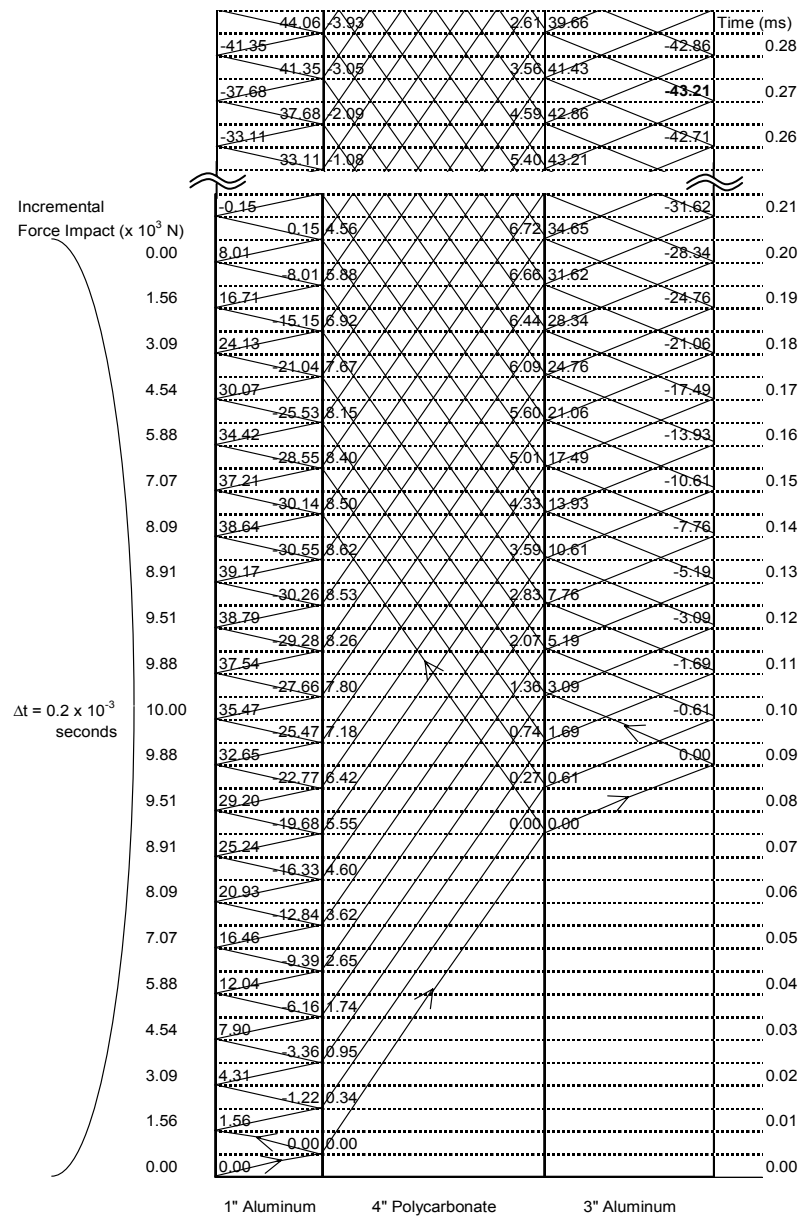


Figure 13. Wave tracing of “APA-1” under a half sine impact with a maximum magnitude of 10×10^3 N and an impact duration of 0.2×10^{-3} seconds. Maximum propagated wave at the right end is 43.21×10^3 N. Column values represent the magnitude of the propagating wave in kN. Positive values indicate a compressive wave and negative tensile.

Acknowledgement

The authors gratefully acknowledge the support of the Army Research Laboratory through the Soldier’s Future Force Electronics Reliability and Survivability Technology Program, cooperative agreement number DAAD19-03-2-0007.

References

- (1) Frost, G. W. and Costello, M. F., Control authority of a projectile equipped with an internal unbalanced part, *Army Research Laboratory*, (2004), ARL-CR-555.
- (2) Wilson, M. J., Hall, R. A. and Ilg, M., ONBORT (On-board Navigation of Ballistic ORDNance): Gun-launched munitions flight controller, *Army Research Laboratory*, (2004), ARL-TR-3210.

- (3) Steinberg, D. S., *Vibration analysis for electronic equipment* (3rd ed.), (2000), New York: John Wiley & Sons, Inc.
- (4) Veprik, A. M. and Babitsky, V. I., Vibration protection of sensitive electronic equipment from harsh harmonic vibration, *Journal of Sound and Vibration*, Vol. 238 (2000), pp. 19-30.
- (5) Chen, P. J. and Gurtin, M. E., On the propagation of one-dimensional acceleration waves in laminated composites, *Journal of Applied Mechanics*, Vol. 40 (1973), pp. 1055-1060.
- (6) Solaroli, G., Gu, Z., Baz, A. and Ruzzene, M., Wave propagation in periodic stiffened shells: spectral finite element modeling and experiments, *Journal of Vibration and Control*, Vol. 9 (2003), pp. 1057-1081.
- (7) Sueki, S., Ladkany, S. G., O'Toole, B. J. and Karpanan, K., Mitigation of high "g" impact vibrations in a projectile using material wave speed mismatch, In G. Kawall, S. Yu and D. Naylor (Eds.), *Proceedings of the 21st Canadian Congress of Applied Mechanics* (2007), pp.776-777.
- (8) Livermore Software Technology Corporation, *LS-DYNA* [computer software], (2006), Livermore, California.
- (9) Altair Engineering, Inc., *Altair HyperWorks 7.0* [computer software], (2004), Troy, Michigan.
- (10) Livermore Software Technology Corporation, *LS-DYNA Keyword user's manual*, Version 970, (2003), Livermore, California.
- (11) Hallquist, J. O. (Comp.), *LS-DYNA Theory manual*, (2005), Livermore, California.
- (12) Thomson, W. T. *Theory of vibration with applications* (4th ed.), (1993), New Jersey: A Simon & Schuster Company.
- (13) Sueki, S. *Mitigation of impact vibration using impedance mismatch in cylindrical structures*, (2009), Doctoral dissertation, University of Nevada, Las Vegas.